Phase segregation dynamics of a chemically reactive binary mixture

Jacob J. Christensen,[1] Ken Elder,[2] and Hans C. Fogedby[1,3]
[1]*Institute of Physics and Astronomy, University of Aarhus, DK-8000 Aarhus C, Denmark*
[2]*Department of Physics, Oakland University, Rochester, Michigan 48309-4401*
[3]*Nordita, Blegdamsvej 17, DK-2100, Copenhagen Ø, Denmark*
(Received 12 January 1996; revised manuscript received 12 March 1996)

We investigate a model system of a chemically reactive binary mixture, where the simple reaction $A \rightleftharpoons B$ between the two constituents of the mixture occurs simultaneously with spinodal decomposition. The competition between the thermodynamic short-range attractive and the reactive long-range repulsive interactions leads to the formation of steady-state patterns. In the case of equal forward and backward reaction rates the steady-state average domain width, R_∞, scales with the reaction rate, Γ, as $R_\infty \sim (1/\Gamma)^s$, where the exponent s equals approximately $\frac{1}{3}$ for low rates and equals exactly $\frac{1}{4}$ for high rates. These exponent values and the variation of the maximum amplitude of the order parameter with the reaction rate can be derived by minimizing the free energy in a square wave and a single mode approximation, respectively. The phase segregation dynamics is simulated numerically using the appropriate Langevin equation. [S1063-651X(96)50509-X]

PACS number(s): 05.70.Fh, 64.60.Cn, 47.54.+r, 61.20.Ja

In recent years there has been a growing interest in physical and chemical systems exhibiting periodic macroscopic patterns and textures. Typical morphologies are stripes, labyrinthine patterns, and circular or spherical droplets which are found in such diverse systems as type I superconductors, Langmuir films, diblock copolymers, and chemical mixtures. The suggested mechanism giving rise to the formation of periodic textures is a competition between interactions of different ranges and strengths favoring spatial inhomogeneities in an otherwise uniform ground state [1].

In this paper we investigate a simple model system, proposed by Glotzer *et al.* [2], of a chemically reactive binary mixture. Here a chemical reaction of the form $A \rightleftharpoons B$ between the two constituents occurs simultaneously with spinodal decomposition [3]. The chemical reaction, which can be identified as an effective long-range repulsive interaction, tends to spatially mix the two components causing the phase separation process to evolve into a labyrinthine steady-state pattern in which the demixing thermodynamic and mixing reactive processes balance. (See Refs. [4,5] for recent experimental and theoretical investigations of similar systems.)

The model is a binary (A-B) mixture described by an order parameter $\phi(\mathbf{r},t)$ $(-1<\phi<1)$, the local concentration difference of the components. When the mixture, initially in a homogeneous equilibrium state, is rapidly cooled (quenched) into the two-phase coexistence region, small inhomogeneities in the order parameter evolve into macroscopic domains of uniform phase $\phi=-1$ or $\phi=1$. The well-known Cahn-Hilliard equation [6] describing the time evolution of the order parameter fluctuations, $\phi(\mathbf{r},t)$, following a critical quench, is extended in order to include the chemical reaction $A \rightleftharpoons B$,

$$\frac{\partial \phi}{\partial t} = M\nabla^2 \frac{\delta F[\phi]}{\delta \phi} - \Gamma_1(1+\phi) + \Gamma_2(1-\phi), \qquad (1)$$

where Γ_1 and Γ_2 denote the forward and backward reaction rates, respectively. Here M is a mobility, and $F[\phi]$ a coarse-grained free energy functional of the Ginzburg-Landau form, $F[\phi]=\int d^d r (f(\phi)+(\kappa/2)(\nabla\phi)^2)$, where κ is a phenomenological constant related to the interaction range. The bulk free energy $f(\phi)$ has the usual double-well structure, $f(\phi)=-(r/2)\phi^2+(u/4)\phi^4$, where r and u are positive phenomenological constants. Since we study the model at zero temperature there is no noise term in Eq. (1) and the statistical nature of the problem appears in the random initial conditions, which have to be averaged over.

Since for unequal rates the system settles in an uninteresting uniform one component phase, we restrict ourselves to the case of equal forward and backward reaction rates. With $\Gamma \equiv \Gamma_1 = \Gamma_2$, Eq. (1) takes the form

$$\frac{\partial \phi}{\partial t} = M\nabla^2 \frac{\delta F[\phi]}{\delta \phi} - 2\Gamma\phi. \qquad (2)$$

As a first observation we notice that for a large reaction rate the reaction term dominates, leading to an exponential decay of the order parameter. Contrary to the demixing caused by the underlying thermodynamics, the effect of the chemical reaction is thus to spatially mix the two components. Formally, the type of interaction introduced by the chemical reaction can be identified by rewriting Eq. (2) as $\partial\phi/\partial t = M\nabla^2 \delta\mathcal{F}[\phi]/\delta\phi$ with the effective free energy [7,8],

$$\mathcal{F}[\phi(\mathbf{r},t)] = F[\phi(\mathbf{r},t)] + \frac{\Gamma}{M}\int\int d^d r d^d r' \, \phi(\mathbf{r},t) G(\mathbf{r},\mathbf{r}') \phi(\mathbf{r}',t), \qquad (3)$$

where $F[\phi]$ is the Ginzburg-Landau functional from above and $G(\mathbf{r},\mathbf{r}')$ is the Green's function defined by the Poisson equation, $\nabla^2 G(\mathbf{r},\mathbf{r}') = -\delta(\mathbf{r}-\mathbf{r}')$. In three dimensions, for example, with suitable boundary conditions, $G(\mathbf{r},\mathbf{r}')$ has the form of a Coulomb potential, $G(\mathbf{r}-\mathbf{r}') = (4\pi|\mathbf{r}-\mathbf{r}'|)^{-1}$. The free energy in Eq. (3) thus contains both a short-range attractive interaction whose strength is controlled by κ, and a nonlocal effective long-range repulsive interaction character-

ized by Γ. As a result the modified Cahn-Hilliard equation [Eq. (2)] describes phase separation in a system with competing interactions [9].

The initial evolution of perturbations in the order parameter is revealed by a linear stability analysis of Eq. (2), [10]. Transforming to dimensionless variables, $\mathbf{r}\rightarrow\sqrt{\kappa/r}\mathbf{r}$, $t\rightarrow(\kappa/2Mr^2)t$, $\phi\rightarrow\sqrt{r/u}\phi$, and $\Gamma\rightarrow(Mr^2/\kappa)\Gamma$, and performing the functional differentiation, Eq. (2) takes the form

$$\frac{\partial\phi}{\partial t}=\frac{1}{2}\nabla^2(-\phi+\phi^3-\nabla^2\phi)-\Gamma\phi. \tag{4}$$

Linearizing in Fourier space about $\phi=0$ one finds that the fluctuations, $\delta\phi_k$, in the order parameter decay exponentially, $\delta\phi_k(t)=\delta\phi_k(0)\exp[-\gamma_k(\Gamma)t]$, with rate $\gamma_k(\Gamma)=1/2(k^4-k^2+2\Gamma)$. Since only k modes with positive $\gamma_k(\Gamma)$ are damped, the roots $k^{\mp}=[\frac{1}{2}(1\mp\sqrt{1-8\Gamma})]^{1/2}$ of $\gamma_k(\Gamma)$ (existing only for $0\leqslant\Gamma\leqslant\frac{1}{8}$) define long and short wavelength cutoffs for the unstable k modes. The former is of greater interest since such a cutoff is not present in the case of spinodal decomposition ($\Gamma=0$). The effect of the long wavelength cutoff is to dampen the soft modes, thus preventing continuing domain coarsening; that is, the phase separation is frozen owing to the presence of the chemical reaction. We notice that $\Gamma=\frac{1}{8}$ is the upper limit for reaction rates allowing phase separation.

We have solved Eq. (4) numerically using a standard finite-difference scheme [11] on two-dimensional lattices of size 256×256. In order to ensure that finite size effects are not relevant, smaller systems were also investigated. Appropriate to a critical quench the system was initially prepared in the homogeneous single phase state by assigning to each lattice site a small random number uniformly distributed about $\phi=0$. We have monitored the time evolution of the patterns formed by calculating the average domain size, $R(t)$, as $2\pi/k^1(t)$, where $k^1(t)=\langle\int dk\,kS(k,t)/\int dk\,S(k,t)\rangle$ is the first moment of the circularly averaged structure factor $S(k,t)$. Here $\langle\rangle$ means an average over random initial conditions implemented by several independent runs. In the absence of the chemical reaction, the system exhibits the usual Lifshitz-Slyozov growth [12] where, at late times after the quench, the characteristic domain size, $R(t)$, scales dynamically as $R(t)\sim t^{1/3}$. In addition, the structure factor satisfies the scaling form, $S(k,t)=R(t)^2g(kR(t))$, which implies that $R(t)$ is the only characteristic length scale in the problem [3]. However, for nonzero reaction rates we observe that the phase separation process is eventually halted, and the system reaches a steady-state configuration with a characteristic time independent domain size, R_∞ (Fig. 1).

The dynamical evolution of the system prior to saturation behaves in two markedly different manners depending on whether the reaction rate is high or low. For low reaction rates the average domain size scales in an intermediate period before saturation approximately as $R(t)\sim t^{1/3}$. For high reaction rates, on the other hand, no such intermediate scaling is observed, as the system rapidly reaches its asymptotic state (Fig. 1). Despite the intermediate scaling of $R(t)$ at low rates we find, however, no evidence that the structure factor satisfies the above-mentioned scaling law for any nonzero

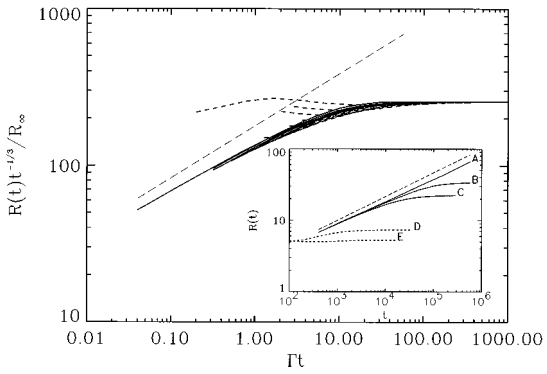

FIG. 1. Test of the scaling form Eq. (5). Low rate systems (solid lines) satisfy the scaling form, whereas the form is violated by high rate systems (dashed lines). The inset shows the time evolution of the average domain size for various values of Γ. *A*: spinodal decomposition. *B* and *C*: low rate systems which scale as $R(t)\sim t^{1/3}$ in an intermediate time period prior to saturation. *D* and *E*: high rate systems which quickly reach the saturation regime. The long-dashed straight lines in both graphs have slope $\frac{1}{3}$.

reaction rates. We interpret this lack of scaling of the structure factor as being due to the presence of several competing length scales [5].

In accordance with Glotzer *et al.* [2] our simulations show that the average width of the steady-state domains scales with the inverse reaction rate as $R_\infty\sim(1/\Gamma)^s$, where the scaling exponent s approaches the value $\frac{1}{3}$ (we find $s=0.29$) for low rates, i.e., $\Gamma\simeq0$. In addition we find that the steady-state systems also exhibit this scaling behavior for high rates, $\Gamma\simeq\frac{1}{8}$, only now with with $s=0.25$ [13]. These exponents have earlier been derived numerically by Liu and Goldenfeld [7] in an investigation of the phase segregation dynamics of a diblock copolymer system which accidentally is governed by an equation of motion identical to Eq. (2).

The dynamical properties of the system, for small reaction rates, can be given a formal description by the introduction of a single scaling form which captures both the dynamical scaling of $R(t)$ and the static scaling of R_∞. The average domain size, $R(t)$, may be written as [7,14]

$$R(t)=t^\alpha F(\Gamma t), \tag{5}$$

where $\alpha=\frac{1}{3}$ is the Lifshitz-Slyozov dynamical scaling exponent, and $F(x)$ is a scaling function with the asymptotic behaviors $F(x)\rightarrow$const, $x\rightarrow0$, and $F(x)\sim x^{-\alpha}$ for $x\gg1$. Then $R(t)\rightarrow R_\infty\sim\Gamma^{-s}$ as $t\rightarrow\infty$ and $R(t)\sim t^\alpha$ for $\Gamma\rightarrow0$. In Fig. 1 we test this scaling form by plotting $\log(R(t)t^{-1/3}/R_\infty)$ versus $\log(\Gamma t)$, and find that systems with sufficiently low rates satisfy this relation, whereas the relation is violated by high rate systems. The values of the reaction rate for which Eq. (5) is satisfied gives rise to the exponent $s=0.29$, whereas the high rates for which Eq. (5) is not obeyed yields the exponent $s=0.25$. Due to the characteristic average domain sizes the scaling regimes corresponding to $s=\frac{1}{3}$ and $s=\frac{1}{4}$ are designated the strong and weak segregation regimes, respectively.

The steady-state systems formed at high rates are characterized by weakly segregated domains with a labyrinthine or stripelike morphology [Fig. 2(b)]. The corresponding struc-

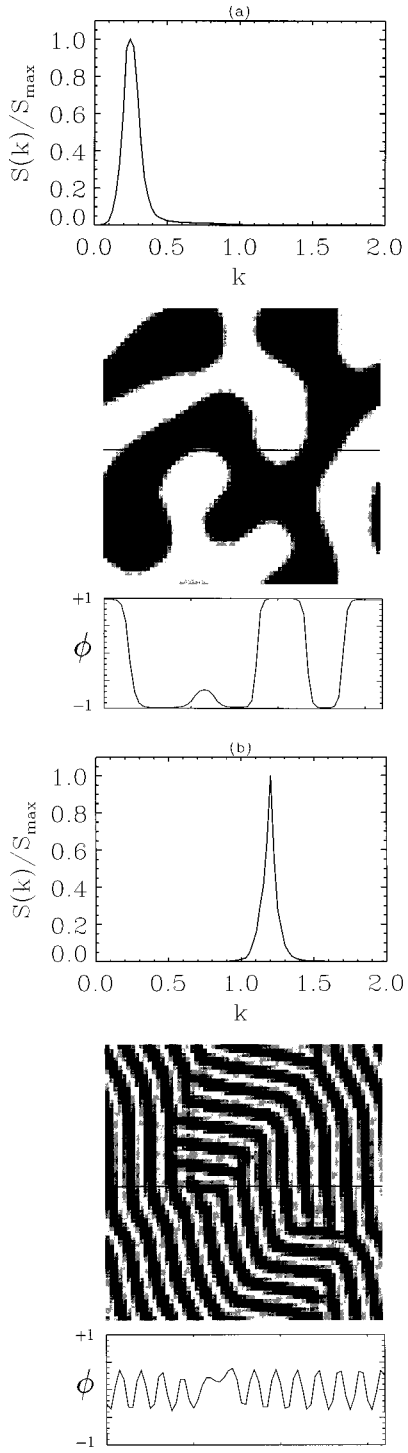

FIG. 2. Steady-state patterns of 64×64 systems, along with their circularly averaged structure factors, and profiles extracted from the lines bisecting the patterns for systems belonging to (a) the strong and (b) the weak segregation regime.

ture factor is very sharply localized, and we therefore propose to describe the steady-state configurations by a single mode approximation, in which the modulation of the order parameter is given by $\phi\sim\cos(kx)$. In addition to the variation of the average domain size with the reaction rate, we also find another functional dependence of Γ. Comparing the profiles of the steady-state patterns for low and high rate systems [Figs. 2(a) and 2(b)], we observe that the maximum

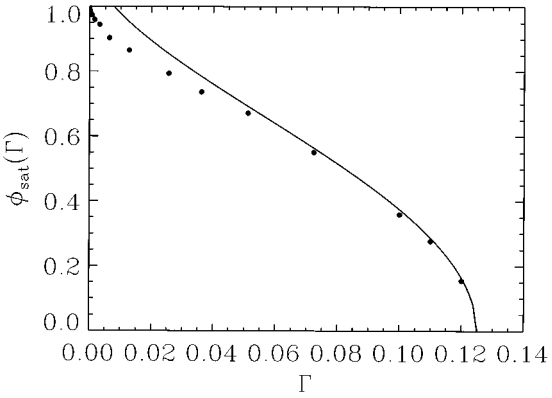

FIG. 3. The behavior of the saturation amplitude as obtained by simulations (●) compared with the analytical expressions obtained in the single mode approximation.

amplitude of the order parameter, the saturation amplitude, decreases with increasing reaction rate. The mixing effect of the chemical reaction tends to diminish the amplitude of the order parameter, whereas the demixing caused by the thermodynamics has the opposite effect on the field amplitude. Thus the value of the saturation amplitude for a given strength of the chemical reaction reflects the level at which these counteracting interactions balance. When the chemical reaction is absent, the saturation amplitude is determined by the minimas of the potential $f(\phi)$ located at $\pm\sqrt{r/u}$, or, expressed in dimensionless variables, at ±1. The initial growth of fluctuations ceases when the order parameter amplitude $|\phi|$ has reached its saturation value ϕ_{sat}. Sharp domain walls are then formed, and further temporal evolution takes place through mutual annihilation of these walls in the process of smaller domains coalescing into larger ones. In the case of spinodal decomposition the saturation amplitude is unity, whereas for nonzero reaction rates we observe a monotonic decrease of the saturation amplitude of the steady-state patterns, as a function of the reaction rate (Fig. 3).

In order to incorporate the variation of the saturation amplitude with the reaction rate, the order parameter at high reaction rates should thus be approximated by the *cosine* form $\phi=\phi_{sat}\cos(kx)$. The dependence of the saturation amplitude and the wave number on the reaction rate can then be determined by substituting the *cosine* ansatz into the free energy expression and minimizing with respect to k and ϕ_{sat}. Using the (1D) dimensionless form of the free energy [Eq. (3)] $\mathcal{F}=\frac{1}{2}\int dx[-\frac{1}{2}\phi^2+\frac{1}{4}\phi^4+\frac{1}{2}(\partial\phi/\partial x)^2]+\Gamma/2\int dx\,dx'\,\phi(x)G(x,x')\phi(x')$, with the Green's function $G(x,x')=0$ and $G(x,x')=(x'-x)$ for $x<x'$ and $x>x'$, respectively, the free energy per volume becomes

$$\mathcal{F}(\phi_{sat},k)=\frac{1}{8}\left[\left(-1+k^2+\frac{2\Gamma}{k^2}\right)\phi_{sat}^2+\frac{3}{8}\phi_{sat}^4\right]. \qquad (6)$$

Determining ϕ_{sat} and k_{sat} by solving $d\mathcal{F}/d\phi_{sat}=0$ and $d\mathcal{F}/dk=0$ yields $k_{sat}=(2\Gamma)^{1/4}$ and $\phi_{sat}(\Gamma)=2\sqrt{1-2\sqrt{2\Gamma}}/\sqrt{3}$. Noting that $R_\infty\sim k_{sat}^{-1}$ we conclude that the single mode approximation correctly reproduces the simulation result $s=\frac{1}{4}$, valid for high reaction rates [15]. The

obtained expression for $\phi_{sat}(\Gamma)$ should be valid for reaction rates near $\frac{1}{8}$, and comparison with simulation data show that this is indeed the case (Fig. 3).

For lower values of Γ the morphology of the steady-state configurations is irregular and the corresponding structure factor contains many modes. The *cosine* approximation is therefore not applicable, as is also revealed by the profile of the low rate system in Fig. 2(b). Ideally one should consider domains separated by an interface described by a hyperbolic tangent profile which is the exact solution in the limit $\Gamma \to 0$, [3]. This, however, complicates the calculations and it is more convenient to approximate an interface by a square wave form, i.e., $\phi(x)=\phi_{sat}[1-2\theta(x-\lambda/2)]$, for $0<x<\lambda$, where $\theta(x)$ is a Heaviside step function. Substituting this expression into the free energy gives

$$\mathcal{F}(\phi_{sat},\lambda)=\frac{1}{2}\left(-\frac{1}{2}+\frac{\Gamma\lambda^2}{12}\right)\phi_{sat}^2+\frac{1}{8}\phi_{sat}^4 + \frac{1}{4\lambda}\int_0^\infty dx\left(\frac{\partial\phi}{\partial x}\right)^2, \tag{7}$$

where the selected wave vector is $k_{sat}=2\pi/\lambda$. The integral over the gradient square term diverges formally for a square wave and we regularize this term by using the hyperbolic tangent profile, $\phi(x)=\phi_{sat}\tanh(x/\zeta)$ at each interface, where $\zeta \to \sqrt{2}$ and $\phi_{sat} \to 1$ in the limit $\Gamma \to 0$. Hence the free energy [Eq. (7)] is

$$\mathcal{F}(\phi_{sat},\lambda)=\frac{1}{2}\left(-\frac{1}{2}+\frac{\Gamma\lambda^2}{12}+\frac{4}{3\zeta\lambda}\right)\phi_{sat}^2+\frac{1}{8}\phi_{sat}^4. \tag{8}$$

Minimizing Eq. (8) with respect to ϕ_{sat} and λ gives $\lambda=2(\Gamma\zeta)^{-1/3}\simeq 2(\sqrt{2}\Gamma)^{-1/3}$ and $\phi_{sat}(\Gamma)=\sqrt{1-(8\Gamma/\zeta^2)^{1/3}} \simeq \sqrt{1-(4\Gamma)^{1/3}}$. Thus, since $\lambda \sim (1/\Gamma)^{1/3}$, the square wave approximation recovers the result $s=\frac{1}{3}$ suggested by numerical work. These results are valid in the strong segregation limit (i.e., $\Gamma \ll 1$) for which $\zeta \ll \lambda$. We conclude by noting that the important difference between the weak and strong segregation limits is that they correspond to an interfacial thickness that is of the order of the selected wavelength ($\zeta \sim \lambda$) and negligible ($\zeta \ll \lambda$), respectively.

In summary, we have identified two segregation regimes characterized by different dynamical evolutions prior to saturation and different scaling exponents for the static scaling of the steady-state domain sizes with the inverse reaction rate. The scaling exponents were derived analytically by minimizing the free energy using the order parameter profiles characterizing each regime. That is a *cosine* and a *square wave* variation for high and low reaction rates, respectively.

J.J.C. and H.C.F. wish to thank Ole G. Mouritsen for attracting our attention to this problem and Alan J. Bray for helpful discussions.

[1] M. Seul and D. Andelman, Science **267**, 476 (1995).
[2] S. C. Glotzer, D. Stauffer, and N. Jan, Phys. Rev. Lett. **72**, 4109 (1994).
[3] For reviews see, e.g., A. J. Bray, Adv. Phys. **43**, 357 (1994); J. D. Gunton, M. S. Miguel, and P. S. Sahni, *Phase Transitions and Critical Phenomena*, edited by C. Domb and J. L. Lebowitz (Academic Press, London, 1983), Vol. 8.
[4] Q. Tran-Cong and A. Harada, Phys. Rev. Lett. **76**, 1162 (1996).
[5] J. Verdasca, P. Borkmans, and G. Dewel, Phys. Rev. E **52**, R4616 (1995).
[6] J. W. Cahn and J. E. Hilliard, J. Chem. Phys. **28**, 258 (1958).
[7] F. Liu and N. Goldenfeld, Phys. Rev. A **39**, 4805 (1989).
[8] S. C. Glotzer and A. Coniglio, Phys. Rev. E **50**, 4241 (1994).
[9] C. Sagui and R. C. Desai, Phys. Rev. E **49**, 2225 (1994).
[10] S. C. Glotzer, E. A. D. Marzio, and M. Muthukumar, Phys. Rev. Lett. **74**, 2034 (1995).
[11] T. M. Rogers, K. Elder, and R. C. Desai, Phys. Rev. B **37**, 9638 (1988).
[12] I. M. Lifshitz and V. V. Slyozov, J. Phys. Chem. Solids **19**, 35 (1961).
[13] The statistical errors in both exponents, $s=0.25$ and $s=0.29$, are insignificant.
[14] S. C. Glotzer, E. A. D. Marzio, and M. Muthukumar, Polym. Mater. Sci. Eng. Proc. Am. Chem. Soc. **71**, 645 (1994).
[15] We notice that the derived scaling exponent is the same as the one found in the spherical approximation of the model investigated by Glotzer and Coniglio [8].